Argon offline-AMS source apportionment of organic aerosol over yearly cycles for an urban, rural and marine site in Northern Europe

C. Bozzetti[1], Y. Sosedova[1], M. Xiao[1], K. R. Daellenbach[1], V. Ulevicius[2], V. Dudoitis[2], G. Mordas[2], S. Byčenkienė[2], K. Plauškaitė[2], A. Vlachou[1], B. Golly[3], B. Chazeau[1], J.-L. Besombes[4], U. Baltensperger[1], J.-L. Jaffrezo[3], J. G. Slowik[1], El Haddad[1], I., and A. S. H. Prévôt[1]

[1] {Laboratory of Atmospheric Chemistry, Paul Scherrer Institute (PSI), 5232 Villigen-PSI, Switzerland}

[2] {Department of Environmental Research, SRI Center for Physical Sciences and Technology, LT-02300 Vilnius, Lithuania}

[3] {Université Grenoble Alpes, CNRS, LGGE, 38000 Grenoble, France}

[4] {Université Savoie Mont-Blanc, LCME, F-73000 Chambéry, France}

Correspondence to: A. S. H. Prévôt (andre.prevot@psi.ch); I. El Haddad (imad.el-haddad@psi.ch)

Supplement of: Argon Offline-AMS source apportionment of organic aerosol over a yearly cycle for 3 different stations in Lithuania

C. Bozzetti et al.

Correspondence to: A. S. H. Prévôt (andre.prevot@psi.ch)

I. El Haddad (imad.el-haddad@psi.ch)

EC:hopanes ratio

The EC:hopanes ratio was calculated considering the sum of the four most abundant measured hopanes (17a(H),21b(H)-norhopane, 17a(H),21b(H)-hopane, 22S,17a(H),21b(H)-

homohopane, and 22R,17a(H),21b(H)-homohopane ($hopanes_{sum}$)). These four hopanes were also the most abundant in the TEOA profiles used in this study to determine the TEOA concentration (He et al., 2006; He et al., 2008; El Haddad et al., 2009; and Fraser et al., 1998).

The EC:hopanes ratio was derived from a multi-parametric fit of EC according to Eq. (S1)

$$EC = a \cdot BBOC + b \cdot hopanes \quad \text{(S1)}$$

where *a* represents EC:BBOC and *b* represents the EC:hopanes ratio. *a* was constrained to 0.39 which is the average EC:BBOC ratio determined from the markers source apportionment.

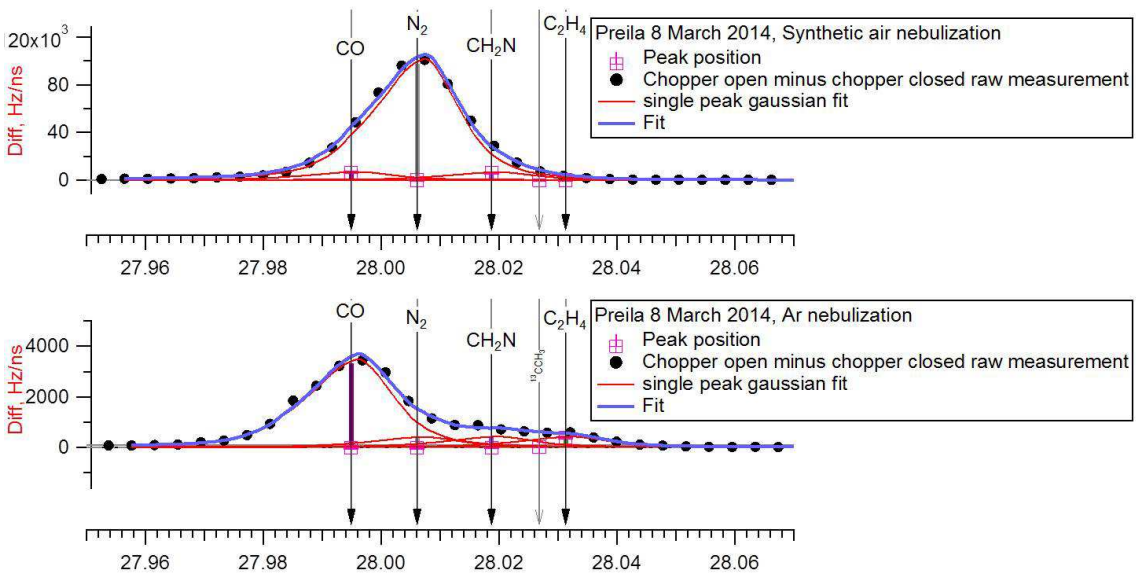

Figure S1. *m/z* 28: HR fit of the chopper open minus closed spectrum (Diff). Top plot: nebulization performed in Ar, bottom plot: nebulization performed in synthetic air.

Table S1: measured compounds.

Compounds class (as in table 1)	**Measured compounds**	**Filters measured**
Ions	SO_4^{2-}, NO_3^-, Cl^-, NH_4^+, Na^+, K^+, Ca^{2+}, Mg^{2+}, oxalate, methane sulfonic acid	All
PAHs	Phenanthrene, anthracene, fluoranthene, pyrene, benzo[a]anthracene, chrysene, triphenylene, retene,	67 composite samples

	benzo[b,k]fluoranthene, benzo[j]fluoranthene, benzo-e-pyrene, benzo[a]pyrene, indeno[1,2,3 -cd]pyrene, dibenzo[a,h]anthracene, benzo[ghi]perylene, coronene
S-PAHs	dibenzothiophene, phenanthro(4,5-bcd)thiophene, Benzo(b)naphtho(2,1-d)thiophene, Benzo(b)naphtha(1,2-d)thiophene Benzo(b)naphtho(2,3-d)thiophene, Dinaphtho(2,1-b;1',2'-d)thiophene, Benzo(b)phenantho(2,1-d)thiophene
Me-PAHs	2-methylnaphtalene, 1-methylfluoranthene, 3-methylphenanthrene, 2-methylphenanthrene, 2-methylanthracene, 4/9 methylphenanthrene, 1-methylphenanthrene, 4-methylpyrene, 1-methylpyrene, 1+3-methylfluoranthene, methylfluoranthene/pyrene, 3-methylchrysene, methylchrysene/benzoanthracene.
Hopanes	Trisnorneohopane, 17a(H)-trisnorhopane, 17a(H),21b(H)-norhopane, 17a(H),21b(H)-hopane, 22S,17a(H),21b(H)-homohopane, 22R,17a(H),21b(H)-homohopane, 22S,17a(H),21b(H)-bishomohopane, 22R,17a(H),21b(H)-bishomohopane, 22S,17a(H),21b(H)-trishomohopane, 22R,17a(H),21b(H)-trishomohopane,
Methoxyphenols	vanillin, vanillic acid, acetovanilone, guaiacyl

	acetone, coniferyl aldehyde, homovanilic acid, syringol, 4-methylsyringol, 4-propenylsyringol, acetosyringone, syringyl acetone, sinapyl aldehyde, syringic acid,	
Others	Cholesterol, 6,10,14-trimethyl-2-pentadecanone	
Sugar alcohols	Arabitol, sorbitol, mannitol	All
Anhydrous sugars	Levoglucosan, mannosan, galactosan	All
Monosaccharides	Glucose	All
Alkanes	Undecane (C11), dodecane (C12), tridecane (C13), tetradecane (C14), pentadecane (C15), exadecane (C16), heptadecane (C17), octadecane (C18), nonadecane (C19), eicosane (C20), heneicosane (C21), docosane (C22), tricosane (C23), tetracosane (C24), pentacosane (C25), hexacosane (C26), heptacosane (C27), octacosane (C28), nonacosane (C29), triacontane (C30), untricontane (C31), totriacontane (C32), tritriacontane (C33), tetratriacontane (C34), pentatriacontane (C35), hexatriacontane (C36), heptatriacontane (C37), octatriacontane (C38), nonatriacontane (C39), tetracontane (C40), pristane, phytane	

1

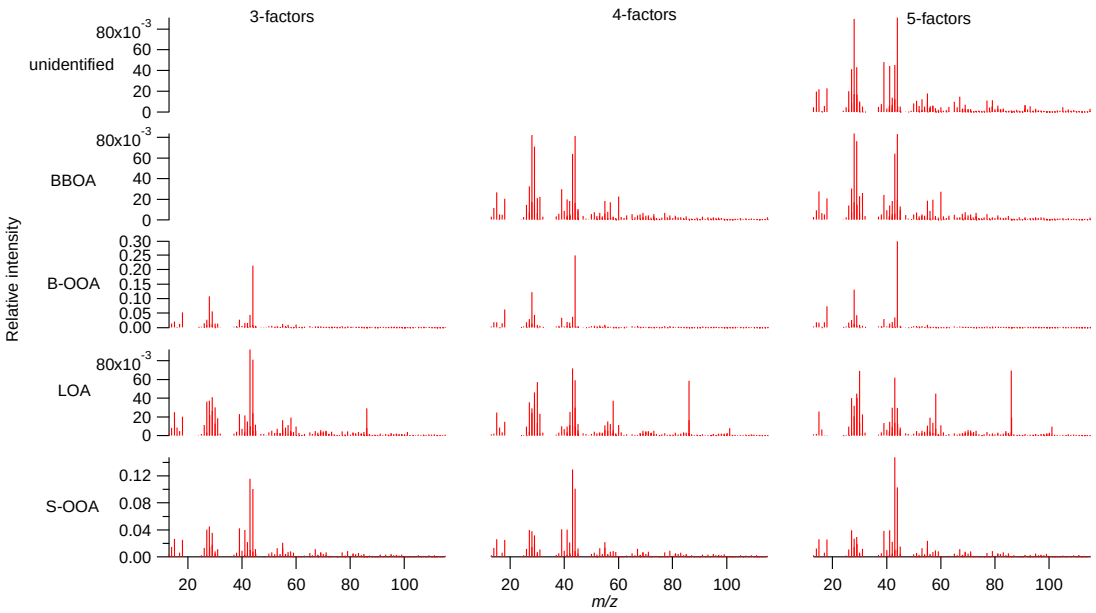

Figure S2. Offline-AMS source apportionment: water-soluble organic aerosol mass spectra of the resolved PMF factors for the 3-, 4-, and 5-factor solutions. The BBOA factor is resolved in the 4-factor solution. Another OOA factor is resolved in the 6-factor solution but could not be associated to a specific aerosol source/process.

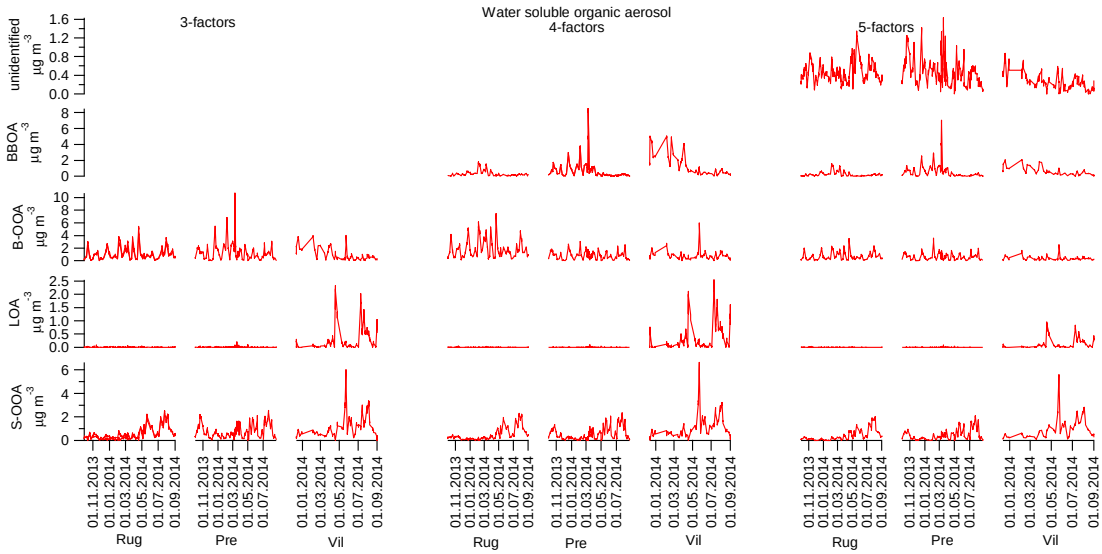

Figure S3. Offline-AMS source apportionment: water-soluble organic aerosol time series of the resolved PMF factors for the 3-, 4-, and 5-factor solutions. The BBOA factor is resolved in the 4- and 5- factor solution.

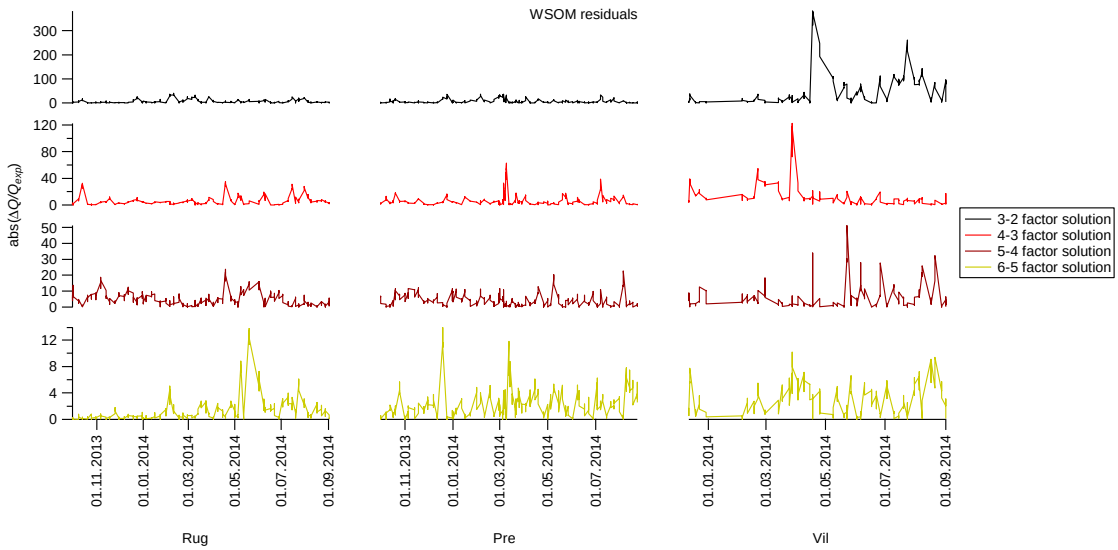

Figure S4. Offline-AMS PMF. Q/Q_{exp} represents the ratio between the sum of the squares of the residuals scaled by the uncertainty (Eq. 2) and the ideal Q (Q_{exp}), which is obtained if the residuals at each point are considered as equal to the uncertainty. Here, abs($\Delta(Q/Q_{exp})$) denotes the absolute difference of Q/Q_{exp} between different solution orders. A strong decrease of the Q/Q_{exp}, passing from lower to higher order solutions indicates a better explanation of the variability by the model. In this study, a large Q/Q_{exp} decrease was observed for Vilnius during summer when passing from 2 to 3 factors, with the separation of the LOA factor. The 4-factor solution enabled resolving BBOA, with a decrease of Q/Q_{exp} observed mostly for Vilnius during winter, where the BBOA concentrations were high. Increasing the number of factors provided further small contributions to the explained variability, resulting in a separation of other OOA factors, which couldn't be associated to aerosol sources or processes.

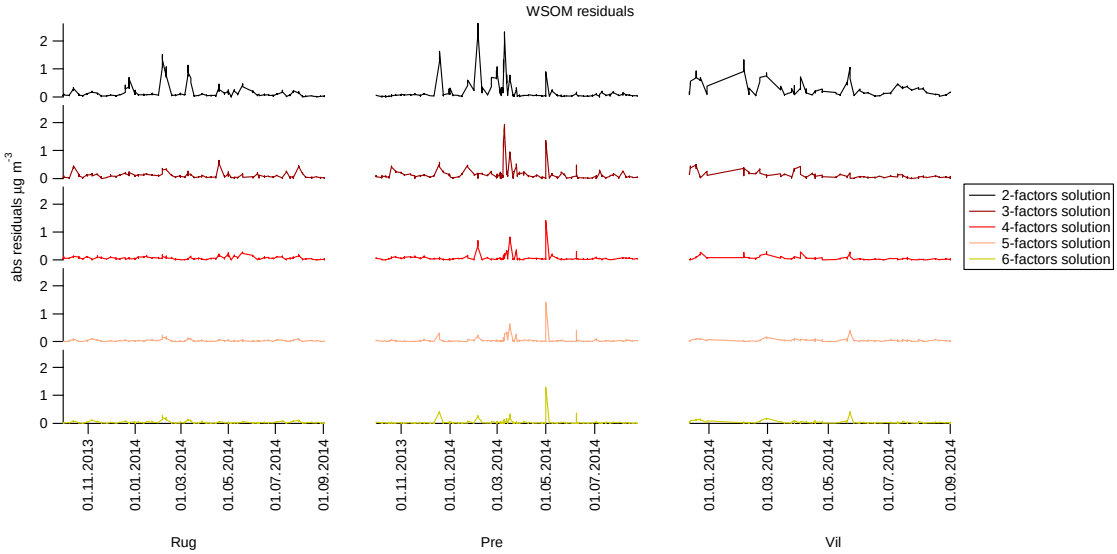

Figure S5. Offline-AMS PMF: WSOM absolute residuals for different number of factors.

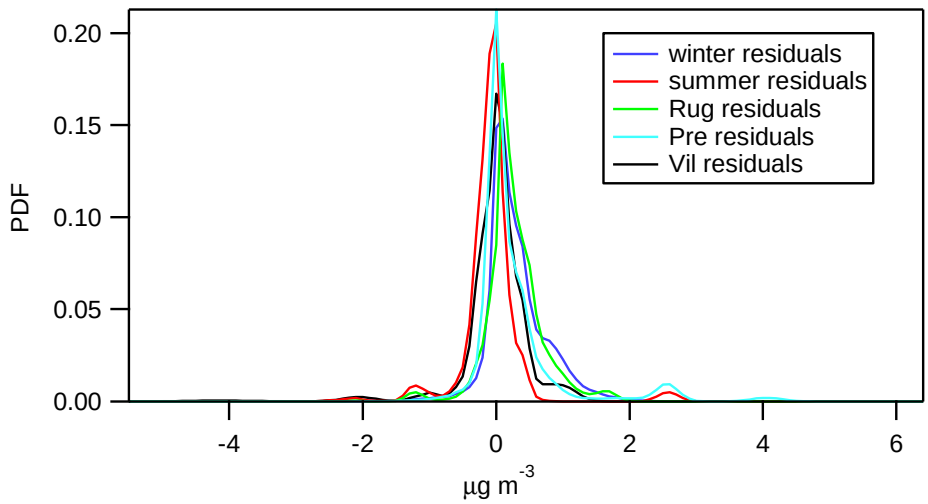

Figure S6. Probability density functions of the OC residuals from R_Z sensitivity analysis (Eq. 6) for different stations and seasons from the accepted solutions (offline-AMS).

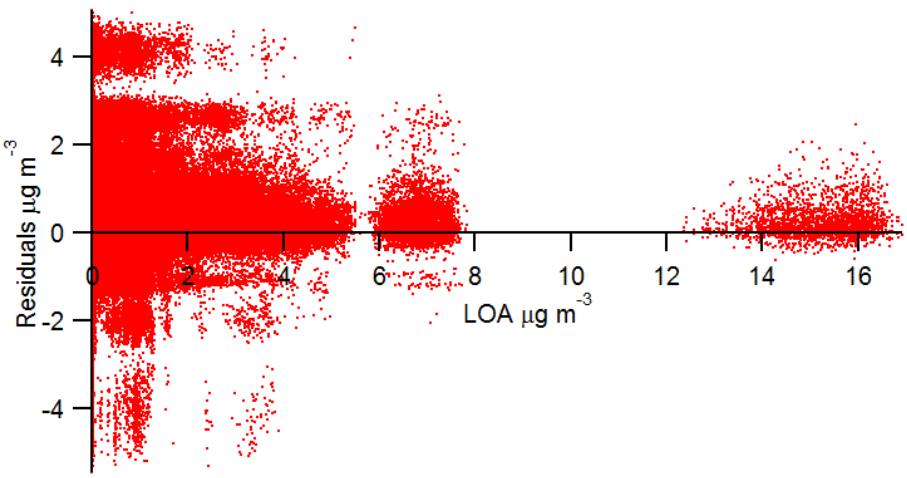

Figure S7. Scatterplot of OC residuals from R_Z sensitivity analysis (Eq. 6) vs LOA concentration from the accepted solutions.

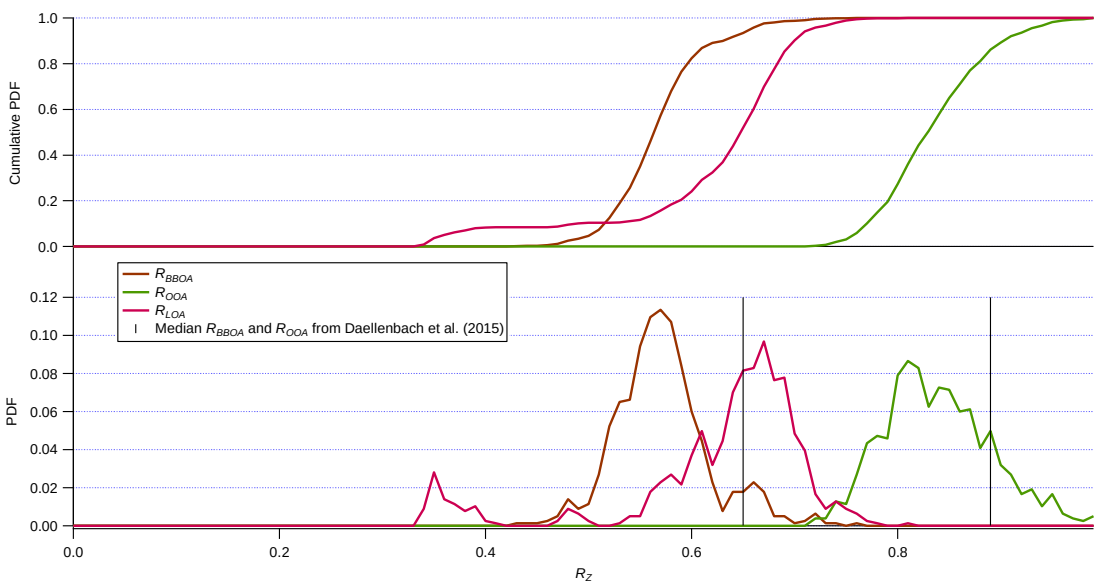

Figure S8. Factor recoveries: probability density functions.

Table S2: *Z*-score table for offline-AMS factor contributions at different stations and seasons. The *z*-score was calculated to determine whether the average factor contribution at one station/season (Z_{avg}) was statistically different from 0.

$$z\text{-}score = Z_{avg}/\sigma_z \quad \text{(S1)}$$

where σ_z denotes the uncertainty calculated according to the source apportionment error model described in the manuscript ($\sigma_{S.A.}$).

Z-score values < 3 are highlighted in pink.

		BBOA	LOA	B-OOA	S-OOA	TEOA
Rug	Fall	13.6	1.8	17.7	8.1	6.1
	winter	21.9	1.9	30.3	7.8	21.2
	spring	9.9	1.9	22.3	15.2	4.3
	summer	10.7	1.6	21.1	15.6	5.7
Pre	Fall	20.6	1.9	19.9	14.3	13.6
	winter	21.1	2.3	22.2	8.7	346.7
	spring	20.6	2.3	21.6	16.9	21.9
	summer	11.5	1.7	15.6	17.1	2.8
Vil	Fall	13.4	1.3	5.3	5.5	23.9
	winter	19.6	1.6	10.4	11.6	30.7
	spring	19.3	2.2	9.2	5.6	36.4
	summer	14.8	4.0	8.7	11.9	10.3

Table S3: *Z*-score table for factor contributions at different stations and seasons (marker source apportionment). Larger uncertainties in comparison to the offline-AMS source apportionment could derive from the smaller amount of variables and measurements. *SA = secondary aerosol. *Z*-score values < 3 are highlighted in pink.

		SO_4^{2-}-SA*	MSA-SA*	NO_3^--SA*	BB	TE	PB	Na^+-rich
Rug	Fall	4.5	0.8	2.6	5.2	1.5	1.1	3.0
	Winter	6.1	1.3	6.8	7.4	2.0	1.9	7.3
	Spring	8.2	1.9	3.7	5.2	1.5	1.4	3.2
	Summer	7.8	1.9	2.0	3.1	1.6	1.7	2.8
Pre	Fall	6.7	1.5	3.6	4.5	1.4	1.8	5.9
	Winter	4.9	1.1	4.5	5.9	1.5	1.4	4.2
	Spring	6.1	3.2	0.9	3.0	1.2	1.4	6.1

	Summer	8.9	3.6	1.5	0.6	1.8	1.9	5.9
Vil	Fall	0.9	1.6	3.9	2.6	0.6	0.7	4.8
	Winter	5.6	0.8	5.6	4.6	1.2	1.2	4.2
	Spring	6.7	1.0	0.7	0.8	0.5	2.1	1.1
	Summer	-	-	-	-	-	-	-

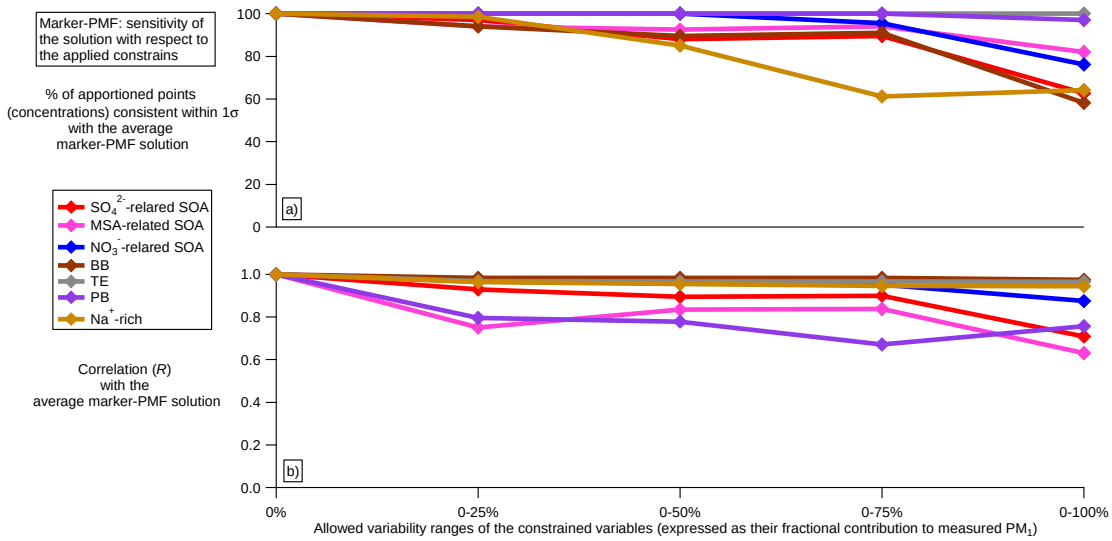

Figure S9. Marker-PMF sensitivity analysis of the applied constraints. Constraints assuming variables to be equal 0 were loosened allowing each of these variables to vary within a certain range of its average relative contribution to measured PM_1. 0% denotes the fully constrained solution, corresponding to the average bootstrap marker-PMF source apportionment.

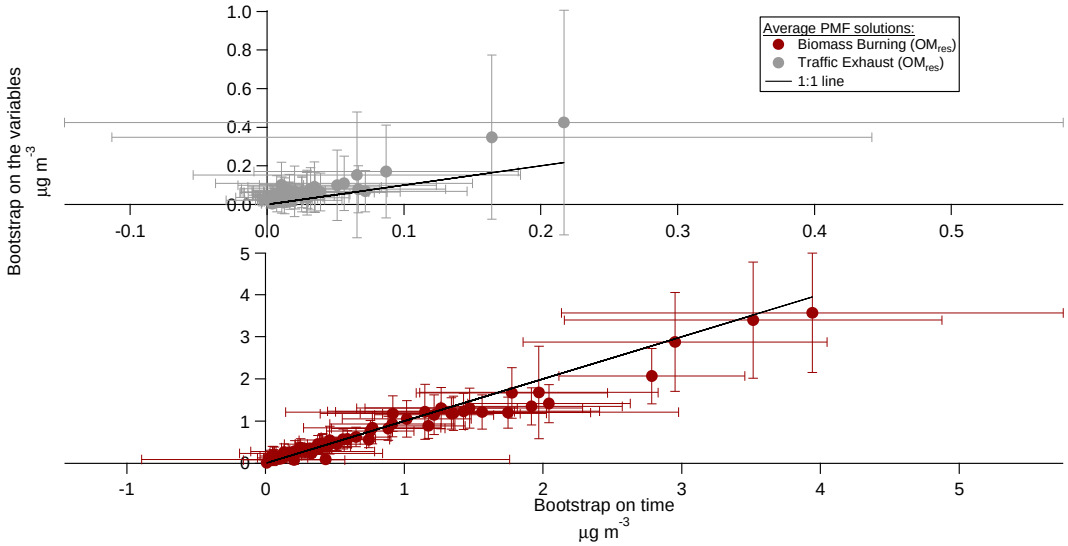

Figure S10. Marker-PMF sensitivity analysis: comparison between the apportionment of OM_{res} in BB and TE obtained bootstrapping time points (x-axes) and variables (y-axes).

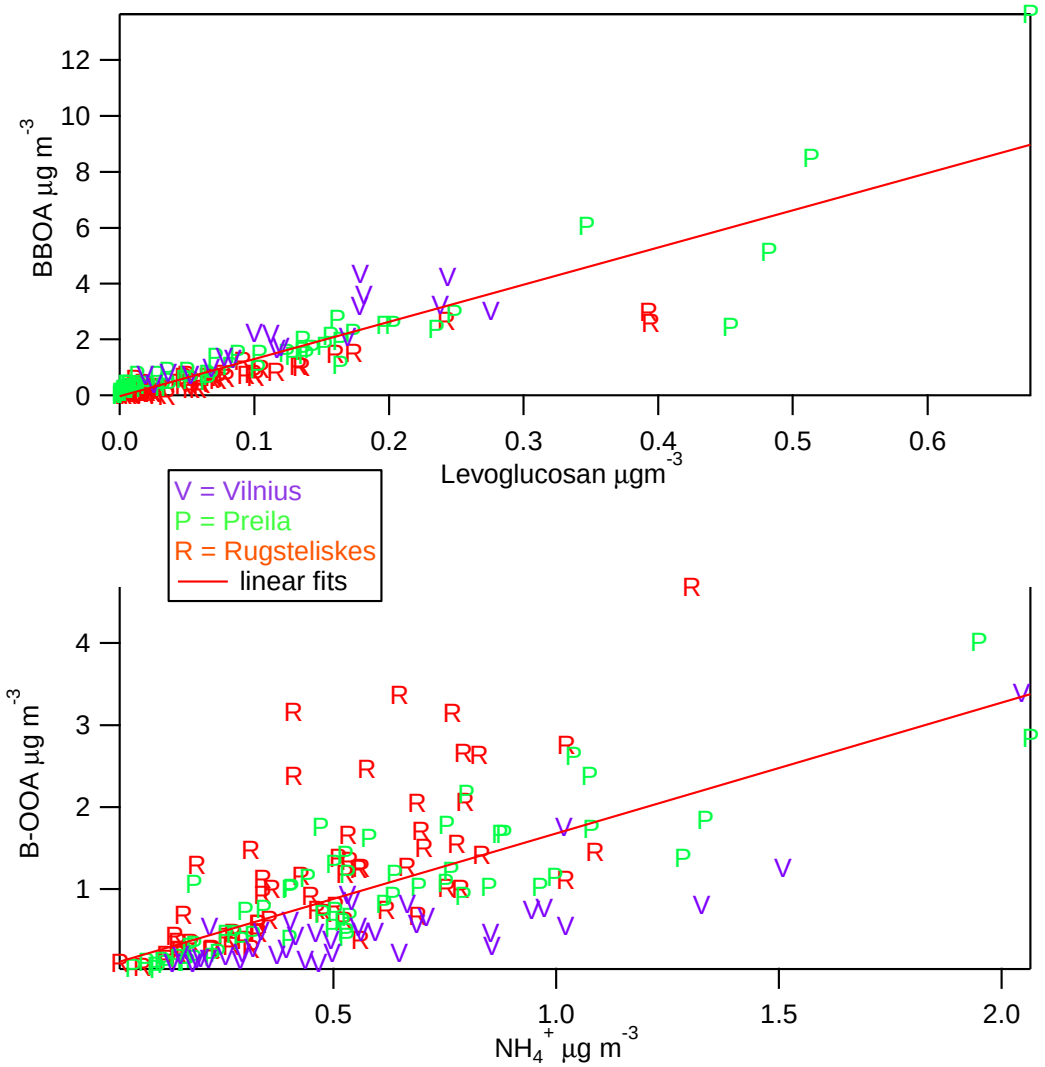

Figure S11. Scatter plots of BBOA vs Levoglucosan (top) and B-OOA vs NH_4^+ (bottom).

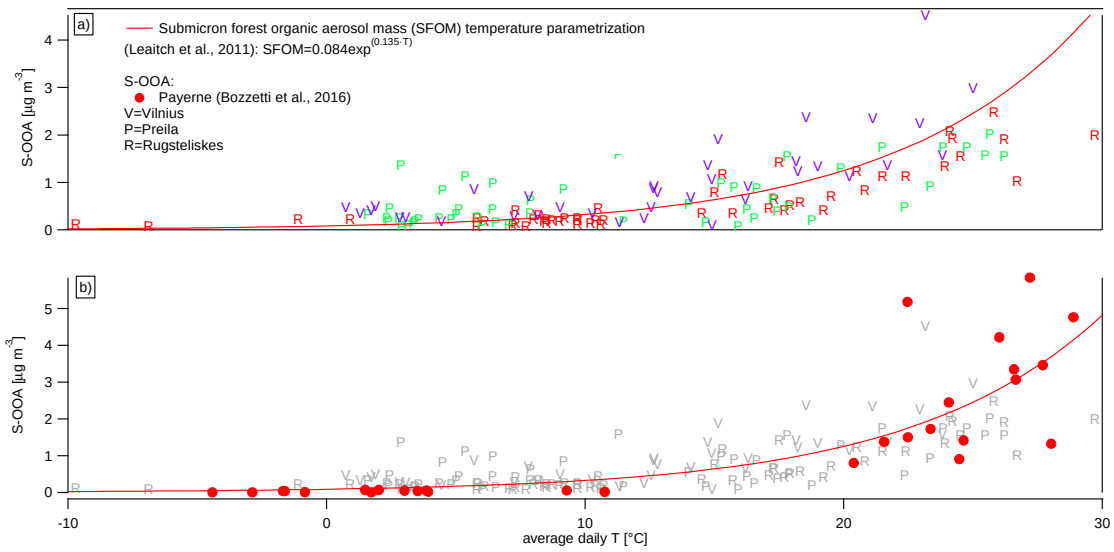

Figure S12. S-OOA temperature dependence and submicron forest organic aerosol mass (SFOM) temperature parameterization by Leaitch et al. (2015). a) Lithuania; b) rural site of Payerne (Switzerland), Bozzetti et al. (2016).

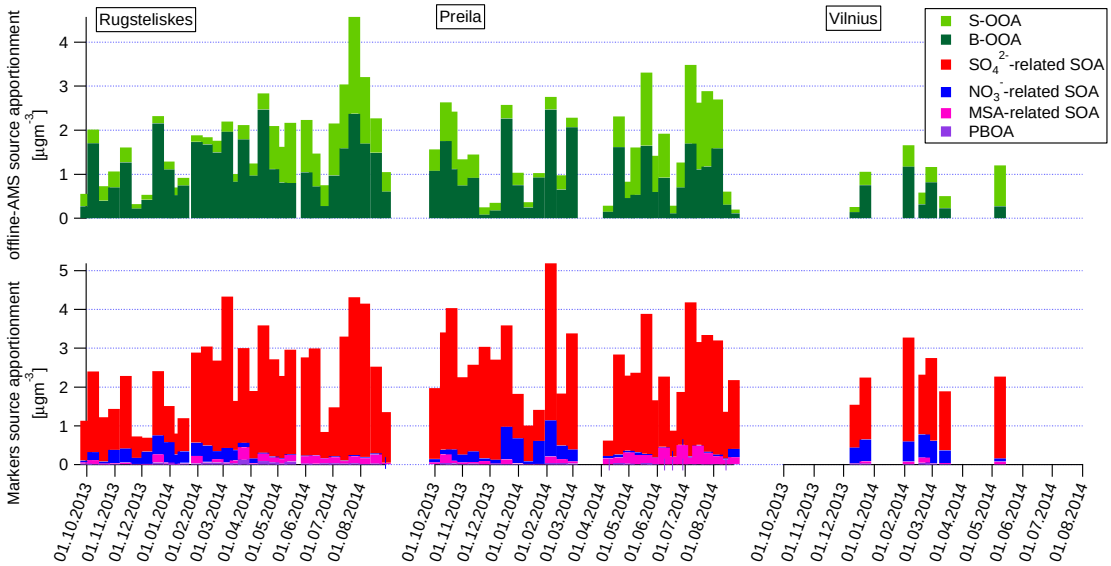

Figure S13. Other-$OA_{offline\text{-}AMS}$ and Other-OA_{marker} time series. Results represent the average PMF solutions.

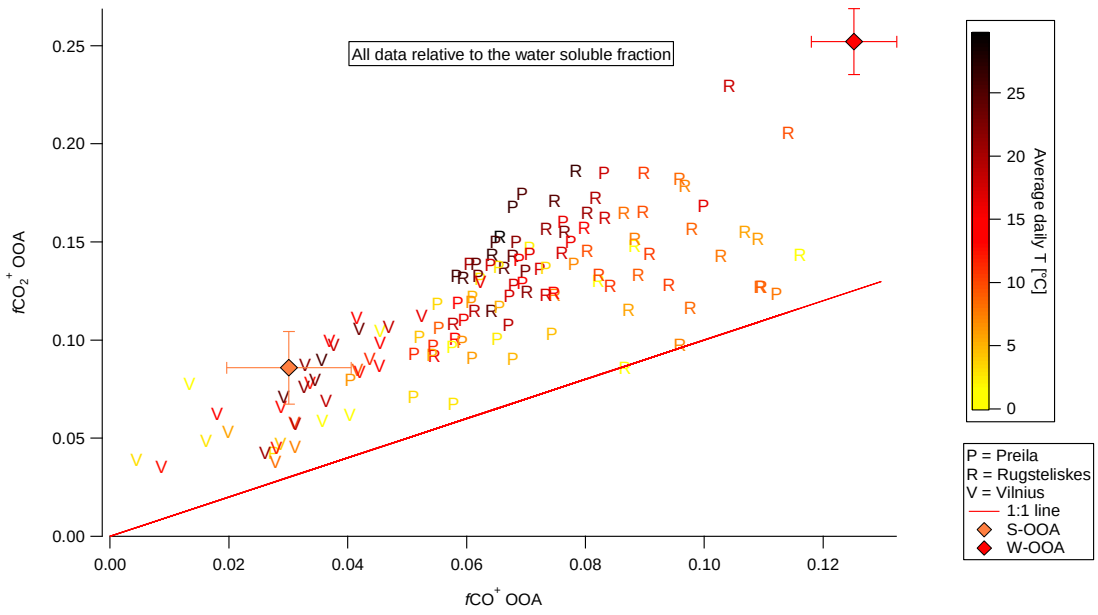

Figure S14. Scatter plot fCO_2^+ *vs.* fCO^+ in water-soluble OOA. The OOA contribution to fCO^+ and fCO_2^+ was estimated by subtracting the non-OOA fCO^+ and fCO_2^+ contributions from the measured fCO^+ and fCO_2^+. The color code denotes the average daily temperature [°C], diamonds indicate the CO_2^+:CO^+ ratio for different PMF factor profiles.

CO^+ parameterization (3-parameter fit)

We fitted the measured water-soluble CO^+ variability as a function of the measured water-soluble CO_2^+, $C_2H_4O_2^+$, and $C_2H_3O^+$. The multilinear fit returned 0.56, 1.30 and -0.18 as coefficients for CO_2^+, $C_2H_4O_2^+$, and $C_2H_3O^+$, respectively. In order to ensure positive contributions from the separated aerosol sources to CO^+, we parameterized the CO^+ variability as the sum of the CO^+ contributions explained by BBOA and S-OOA and B-OOA, which together represented 97% of the CO^+ explained variability (BBOA 20%, S-OOA 12%, B-OOA 65%):

$$CO^+_i = CO^+_{S\text{-}OOA,i} + CO^+_{B\text{-}OOA,i} + CO^+_{BBOA,i} \quad \text{(S3)}$$

The CO^+_i parameterization as a function of the CO^+ fraction explained by the PMF factors ensures positive contributions from all terms.

The $CO^+_{S\text{-}OOA,i}$, $CO^+_{B\text{-}OOA,i}$, and $CO^+_{BBOA,i}$ terms can be written as functions of CO_2^+, $C_2H_3O^+$, and $C_2H_4O_2^+$, chosen as S-OOA, B-OOA, and BBOA tracers.

$$CO^+_{S\text{-}OOA,i} = \left(\frac{fCO^+}{fC_2H_3O^+}\right)_{S-OOA} \cdot C_2H_3O^+_{S-OOA,i} \quad \text{(S4)}$$

$$CO^{+}_{B\text{-}OOA,i} = \left(\frac{fCO^{+}}{fCO_2^{+}}\right)_{B-OOA} \cdot CO_2^{+}{}_{B-OOA,i} \tag{S5}$$

$$CO^{+}_{BBOA,i} = \left(\frac{fCO^{+}}{fC_2H_4O_2^{+}}\right)_{BBOA} \cdot C_2H_4O_2^{+}{}_{BBOA,i} \tag{S6}$$

Therefore Eq. (S3) can be expressed as:

$$CO^{+}_{i} = \left(\frac{fCO^{+}}{fC_2H_3O^{+}}\right)_{S-OOA} \cdot C_2H_3O^{+}{}_{S-OOA,i} + CO^{+}_{B\text{-}OOA,i} + \left(\frac{fCO^{+}}{fCO_2^{+}}\right)_{B-OOA} \cdot CO_2^{+}{}_{B-OOA,i} + CO^{+}_{BBOA,i} + \left(\frac{fCO^{+}}{fC_2H_4O_2^{+}}\right)_{BBOA} \cdot C_2H_4O_2^{+}{}_{BBOA,i} \tag{S7}$$

Then $C_2H_3O^{+}_{S\text{-}OOA,i}$, $C_2H_4O_2^{+}{}_{BBOA,i}$, $CO_2^{+}{}_{B\text{-}OOA,i}$ can be written as the difference between the total fragment concentrations minus the fragment concentrations explained by the other PMF factors:

$$C_2H_3O^{+}_{S\text{-}OOA,i} = C_2H_3O^{+}_{i} - C_2H_3O^{+}_{BBOA,i} - C_2H_3O^{+}_{B\text{-}OOA,i} \tag{S8}$$

$$C_2H_4O_2^{+}{}_{BBOA,i} = C_2H_4O_2^{+}{}_{i} - C_2H_4O_2^{+}{}_{S\text{-}OOA,i} - C_2H_4O_2^{+}{}_{B\text{-}OOA,i} \tag{S9}$$

$$CO_2^{+}{}_{B\text{-}OOA,i} = CO_2^{+}{}_{i} - CO_2^{+}{}_{S\text{-}OOA,i} - CO_2^{+}{}_{BBOA,i} \tag{S10}$$

By substituting Eq. (S9), Eq. (S10), and Eq. (S11) into Eq. (S7) and grouping the CO_2^{+}, $C_2H_4O_2^{+}$, and $C_2H_3O^{+}$ multiplication coefficients, we can express the CO^{+}_{i} variability as function of the $C_2H_3O^{+}$, $C_2H_4O_2^{+}$, and CO_2^{+} fragments as:

$$CO^{+}_{i} = a \cdot CO_2^{+}{}_{i} + b \cdot C_2H_4O_2^{+}{}_{i} + c \cdot C_2H_3O^{+}_{i} \tag{S10}$$

Algebraic expressions for the pre-factors *a*, *b*, and *c* are given in Eq. (S11), (S12) and (S13). These coefficients were estimated as equal to 0.51, 1.50, and -0.10, respectively.

$$a = \frac{-\left(\frac{CO^{+}}{C_2H_4O_2^{+}}\right)_{S\text{-}OOA}\left(\frac{C_2H_4O_2^{+}}{CO_2^{+}}\right)_{B\text{-}OOA} + \left(\frac{C_2H_3O^{+}}{C_2H_4O_2^{+}}\right)_{BBOA}\left(\frac{C_2H_4O_2^{+}}{CO_2^{+}}\right)_{B\text{-}OOA}\left(\frac{CO^{+}}{C_2H_3O^{+}}\right)_{S\text{-}OOA} - \left(\frac{CO^{+}}{CO_2^{+}}\right)_{B\text{-}OOA} - \left(\frac{C_2H_3O^{+}}{C_2H_4O_2^{+}}\right)_{BBOA}\left(\frac{C_2H_4O_2^{+}}{C_2H_3O^{+}}\right)_{S\text{-}OOA}\left(\frac{CO^{+}}{CO_2^{+}}\right)_{B\text{-}OOA} - \left(\frac{C_2H_4O_2^{+}}{CO_2^{+}}\right)_{B\text{-}OOA}\left(\frac{CO_2^{+}}{C_2H_4O_2^{+}}\right)_{BBOA} + \left(\frac{CO_2^{+}}{C_2H_3O^{+}}\right)_{S\text{-}OOA}\left(\frac{C_2H_3O^{+}}{CO_2^{+}}\right)_{B\text{-}OOA}\left(\frac{CO^{+}}{C_2H_4O_2^{+}}\right)_{BBOA}}{-\left(\frac{C_2H_3O^{+}}{CO_2^{+}}\right)_{B\text{-}OOA}\left(\frac{CO_2^{+}}{C_2H_3O^{+}}\right)_{S\text{-}OOA} - \left(\frac{CO_2^{+}}{C_2H_4O_2^{+}}\right)_{BBOA}\left(\frac{C_2H_4O_2^{+}}{CO_2^{+}}\right)_{B\text{-}OOA} + \left(\frac{C_2H_3O^{+}}{C_2H_4O_2^{+}}\right)_{BBOA}\left(\frac{CO_2^{+}}{C_2H_3O^{+}}\right)_{S\text{-}OOA}\left(\frac{C_2H_4O_2^{+}}{CO_2^{+}}\right)_{B\text{-}OOA} + \left(\frac{C_2H_3O^{+}}{CO_2^{+}}\right)_{B\text{-}OOA}\left(\frac{CO_2^{+}}{C_2H_4O_2^{+}}\right)_{BBOA}\left(\frac{C_2H_4O_2^{+}}{C_2H_3O^{+}}\right)_{B\text{-}OOA} - \left(\frac{C_2H_3O^{+}}{C_2H_3O^{+}}\right)_{BBOA}\left(\frac{C_2H_4O_2^{+}}{C_2H_3O^{+}}\right)_{S\text{-}OOA} + 1} \tag{S11}$$

$$b = \frac{-\left(\frac{CO^{+}}{C_2H_3O^{+}}\right)_{S\text{-}OOA}\left(\frac{C_2H_3O^{+}}{C_2H_4O_2^{+}}\right)_{BBOA} + \left(\frac{CO^{+}}{C_2H_3O^{+}}\right)_{S\text{-}OOA}\left(\frac{C_2H_3O^{+}}{CO_2^{+}}\right)_{B\text{-}OOA}\left(\frac{CO_2^{+}}{C_2H_4O_2^{+}}\right)_{BBOA} - \left(\frac{CO^{+}}{CO_2^{+}}\right)_{B\text{-}OOA}\left(\frac{CO_2^{+}}{C_2H_4O_2^{+}}\right)_{BBOA} + \left(\frac{CO^{+}}{CO_2^{+}}\right)_{B\text{-}OOA}\left(\frac{CO_2^{+}}{C_2H_3O^{+}}\right)_{S\text{-}OOA}\left(\frac{C_2H_3O^{+}}{C_2H_4O_2^{+}}\right)_{BBOA} + \left(\frac{CO^{+}}{C_2H_4O_2^{+}}\right)_{BBOA} - \left(\frac{CO^{+}}{C_2H_4O_2^{+}}\right)_{BBOA}\left(\frac{C_2H_3O^{+}}{CO_2^{+}}\right)_{B\text{-}OOA}\left(\frac{CO_2^{+}}{C_2H_3O^{+}}\right)_{S\text{-}OOA}}{-\left(\frac{C_2H_3O^{+}}{CO_2^{+}}\right)_{B\text{-}OOA}\left(\frac{CO_2^{+}}{C_2H_3O^{+}}\right)_{S\text{-}OOA} - \left(\frac{CO_2^{+}}{C_2H_4O_2^{+}}\right)_{BBOA}\left(\frac{C_2H_4O_2^{+}}{CO_2^{+}}\right)_{B\text{-}OOA} + \left(\frac{C_2H_3O^{+}}{C_2H_4O_2^{+}}\right)_{BBOA}\left(\frac{CO_2^{+}}{C_2H_3O^{+}}\right)_{S\text{-}OOA}\left(\frac{C_2H_4O_2^{+}}{CO_2^{+}}\right)_{B\text{-}OOA} + \left(\frac{C_2H_3O^{+}}{CO_2^{+}}\right)_{B\text{-}OOA}\left(\frac{CO_2^{+}}{C_2H_4O_2^{+}}\right)_{BBOA}\left(\frac{C_2H_4O_2^{+}}{C_2H_3O^{+}}\right)_{B\text{-}OOA} - \left(\frac{C_2H_3O^{+}}{C_2H_3O^{+}}\right)_{BBOA}\left(\frac{C_2H_4O_2^{+}}{C_2H_3O^{+}}\right)_{S\text{-}OOA} + 1} \tag{S12}$$

$$c = \frac{\left(\frac{CO^{+}}{C_2H_3O^{+}}\right)_{S\text{-}OOA} - \left(\frac{CO^{+}}{C_2H_3O^{+}}\right)_{S\text{-}OOA}\left(\frac{CO^{+}}{CO_2^{+}}\right)_{B\text{-}OOA} - \left(\frac{CO_2^{+}}{C_2H_4O_2^{+}}\right)_{BBOA}\left(\frac{C_2H_4O_2^{+}}{CO_2^{+}}\right)_{B\text{-}OOA}\left(\frac{CO^{+}}{C_2H_3O^{+}}\right)_{S\text{-}OOA} + \left(\frac{CO^{+}}{CO_2^{+}}\right)_{B\text{-}OOA}\left(\frac{CO_2^{+}}{C_2H_4O_2^{+}}\right)_{BBOA}\left(\frac{C_2H_4O_2^{+}}{C_2H_3O^{+}}\right)_{B\text{-}OOA} + \left(\frac{CO_2^{+}}{C_2H_3O^{+}}\right)_{S\text{-}OOA}\left(\frac{CO^{+}}{C_2H_4O_2^{+}}\right)_{BBOA}\left(\frac{C_2H_4O_2^{+}}{CO_2^{+}}\right)_{B\text{-}OOA} - \left(\frac{CO^{+}}{C_2H_4O_2^{+}}\right)_{BBOA}\left(\frac{C_2H_4O_2^{+}}{C_2H_3O^{+}}\right)_{S\text{-}OOA}}{-\left(\frac{C_2H_3O^{+}}{CO_2^{+}}\right)_{B\text{-}OOA}\left(\frac{CO_2^{+}}{C_2H_3O^{+}}\right)_{S\text{-}OOA} - \left(\frac{CO_2^{+}}{C_2H_4O_2^{+}}\right)_{BBOA}\left(\frac{C_2H_4O_2^{+}}{CO_2^{+}}\right)_{B\text{-}OOA} + \left(\frac{C_2H_3O^{+}}{C_2H_4O_2^{+}}\right)_{BBOA}\left(\frac{CO_2^{+}}{C_2H_3O^{+}}\right)_{S\text{-}OOA}\left(\frac{C_2H_4O_2^{+}}{CO_2^{+}}\right)_{B\text{-}OOA} + \left(\frac{C_2H_3O^{+}}{CO_2^{+}}\right)_{B\text{-}OOA}\left(\frac{CO_2^{+}}{C_2H_4O_2^{+}}\right)_{BBOA}\left(\frac{C_2H_4O_2^{+}}{C_2H_3O^{+}}\right)_{B\text{-}OOA} - \left(\frac{C_2H_3O^{+}}{C_2H_3O^{+}}\right)_{BBOA}\left(\frac{C_2H_4O_2^{+}}{C_2H_3O^{+}}\right)_{S\text{-}OOA} + 1} \tag{S13}$$

Limitations of this parameterization could arise in case of dominating COA contributions, such as in direct emission studies, as the typical AMS fingerprint associated to this source

shows high $fC_2H_3O^+$ and low fCO_2^+ and $fC_2H_4O_2^+$ contributions, leading to a possible negative fCO^+ estimate.

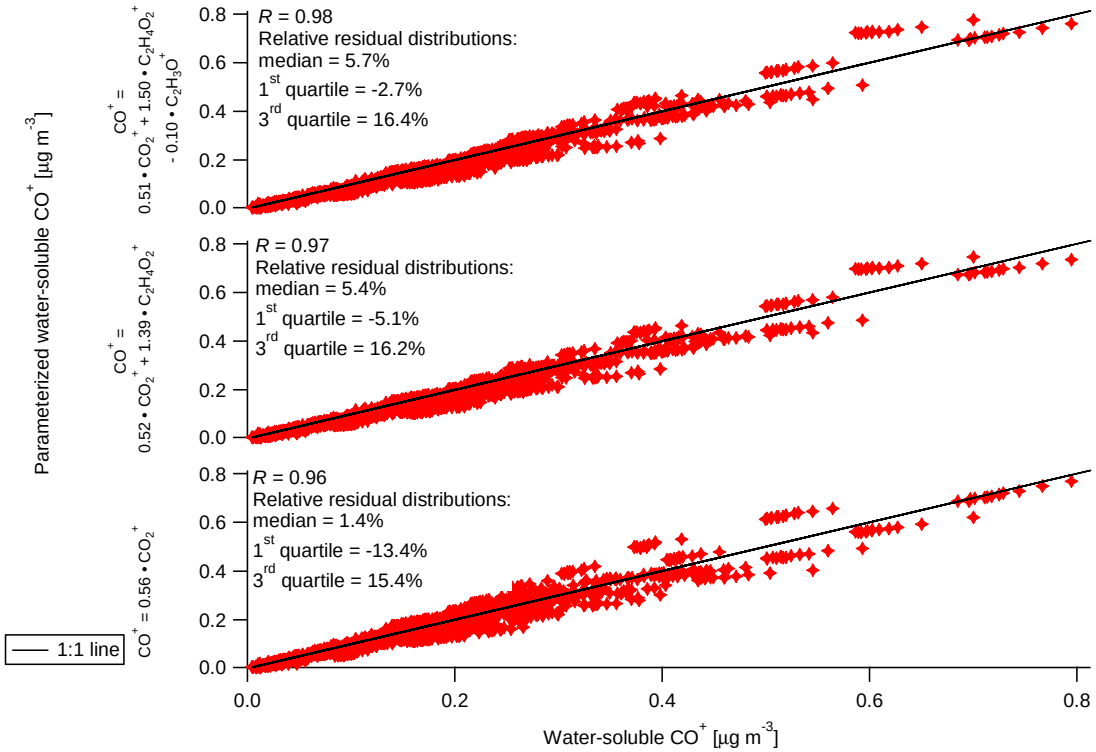

Figure S15. CO^+ parameterization residuals: 1, 2, and 3-parameters fit.